Chemical Methodologies 2(2018) 223-238

Chemical Methodologies

Journal homepage: http://chemmethod.com

Original Research article

Insight into the Stability, Reactivity, Structural and Spectral Properties of the Anti, Syn-endo and Syn-exo Isomers of Bis(*N*-ethoxy-*N*-ethyl-dithiocarbamato)Nitrido Technetium-99m [^{99m}Tc-N(NOEt)$_2$] Radiopharmaceutical

Mehdi Nabati*

Synthesis and Molecular Simulation Laboratory, Chemistry Department, Pars Isotope Company, P.O. Box: 1437663181, Tehran, Iran

ARTICLE INFORMATION

Received: 17 March 2018
Received in revised: 27 April 2018
Accepted: 21 May 2018
Available online: 01 July 2018

DOI:
10.22631/chemm.2018.125281.1043

KEYWORDS

Coronary artery disease
Density functional theory
Nuclear medicine
Radiopharmaceutical
^{99m}Tc-N(NOEt)$_2$

ABSTRACT

(Ethoxy(ethyl)amino)methanedithiol is used in nuclear medicines as a ligand for the preparation of diagnostic radiopharmaceuticals. Among the available radionuclide tracers, technetium-99m (^{99m}Tc) is a good choice for myocardial perfusion imaging. Among the various cardiac perfusion imaging agents, bis(*N*-ethoxy-*N*-ethyl-dithiocarbamato)nitride technetium-99m radiopharmaceutical has a very high uptake. During the present study, the reactivity, stability, structural and spectral properties of anti, syn-endo and syn-exo isomers of bis(*N*-ethoxy-*N*-ethyl-dithiocarbamato)nitride technetium-99m radiopharmaceutical were discussed by density functional theory (DFT) computational method. It can be deduced from the theoretically applied computations that the anti-molecular structure is generally more stable than the syn-endo- and syn-exo- ones.

*Corresponding author, email: mnabati@ymail.com
Synthesis and Molecular Simulation Laboratory, Chemistry Department, Pars Isotope Company, P.O. Box: 1437663181, Tehran, Iran. tel: +982188337023, Fax number: +982188337024

Graphical Abstract

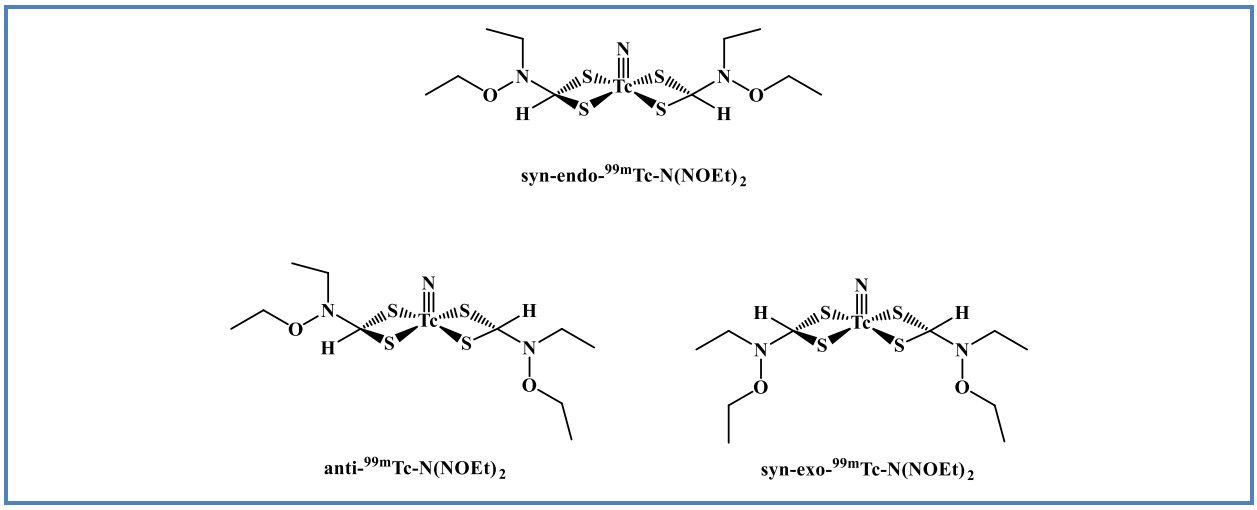

Introduction

The most famous type of the heart diseases is related to the coronary artery disease (CAD) [1]. The main reason of this disease is hard pumping of blood tothe heart muscle. This happens when the various materials such as cholesterol cover the inner walls of the blood vessels. These materials are called plaque. The big plaques (atherosclerosis) cause the slow flowing of the blood through the arteries [2-4]. So, the heart muscle encounters a lack of oxygen and blood. This problem causes a heart attack or an angina (chest pain). In some cases, the coronary artery disease (CAD) contributes to arrhythmias and heart failure. The pharmacological stress myocardial perfusion imaging is used for the CAD detection. Therefore, selection of the best pharmacological stressors and radionuclides is more important to access the optimal perfusion imaging protocol [5-8]. Among the available radionuclide tracers, technetium-99m (^{99m}Tc) is a good choice for myocardial perfusion imaging [9]. In this sense, among the various cardiac perfusion imaging agents, bis(*N*-ethoxy-*N*-ethyl-dithiocarbamato)nitride technetium-99m radiopharmaceutical has a very high uptake [10-13]. This nuclear medicine is a novel member of the neutral myocardial perfusion imaging agents [14]. The mentioned nuclear compound has lipophilic molecular structure and is rapidly extracted by myocardium in dogs, rats, monkeys, rabbits and human beings. The kit formulation of this radiopharmaceutical is very easy [15]. So, it can be easily used for diagnosis of the coronary artery disease. In recent years, many preclinical and clinical works have been done on ^{99m}Tc-N(NOEt)$_2$ imaging agent [16-18]. It has been proved that ^{99m}Tc-N(NOEt)$_2$ has superior properties for imaging myocardial ischemia than hexakis-2-methoxyisobutylisonitrile technetium-99m (^{99m}Tc-MIBI) [19]. Also, it has shown good responses in tumor imaging and detection of tumor cells [20]. Unfortunately, in our best studies, the chemical structure of this radiopharmaceutical has not been

taken into consideration. During the present research, we theoretically study and investigate the stability, reactivity, and structural and spectral properties of the ^{99m}Tc-N(NOEt)$_2$ myocardial perfusion imaging agent. In order to better understand the real structure of this radiopharmaceutical, its different isomers (anti, syn-endo and syn-exo) are discussed. We use the density functional theory (DFT) computational method for our studies.

Materials and methods

During the present research, the quantum mechanical computationswere done and themolecular structures of anti, syn-endo and syn-exoisomers of bis(*N*-ethoxy-*N*-ethyl-dithiocarbamato)nitride technetium-99m radiopharmaceutical were optimized using density functional theory (DFT) method (B3LYP functional) with cc-pVDZ basis set of theory by the Gaussian 03W program package [21-23]. The Lanl2DZ basis set was used to the computation of technetium-99m radionuclide. Also, the ChemBioDraw Ultra 13.0, GaussView 6.0.16 and GaussSum 3.0 programs were used for drawing molecules, visualizing molecular structures and obtaining spectral graphs, respectively. After optimizing the structures, the vibrational frequencies were computed for all molecules. It is worth mentioning that there was not any imaginary frequency for all isomers. So, it proves the accuracy of our computations.

Results and discussion

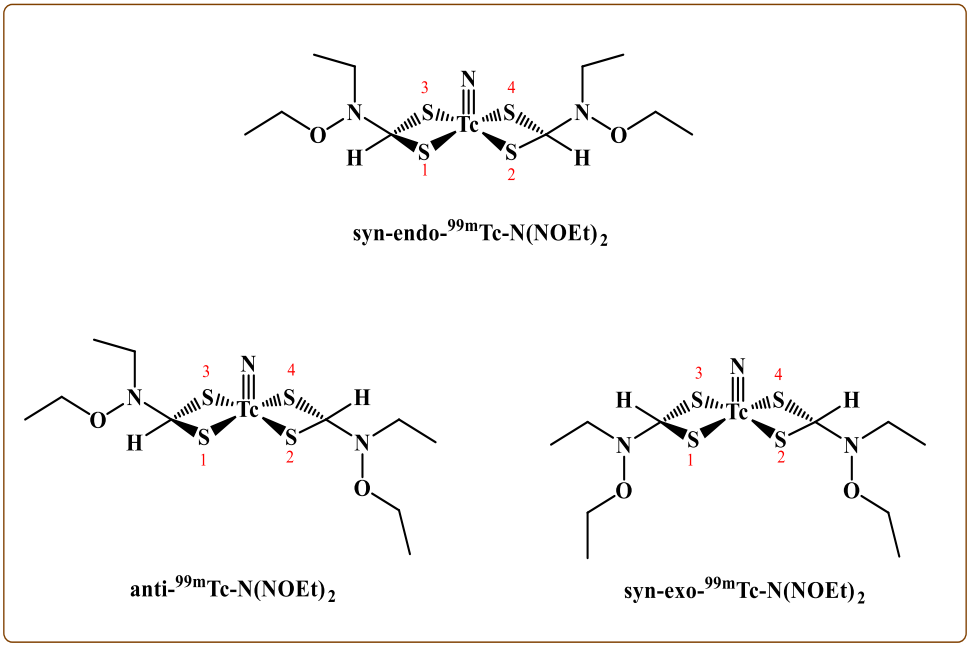

Scheme 1. Molecular structure of ^{99m}Tc-N(NOEt)$_2$ isomers.

Scheme 1 shows the molecular structure of the isomers of ^{99m}Tc-N(NOEt)$_2$ radiopharmaceutical. As it can be seen two (ethoxy(ethyl)amino) methanedithiol ligands have been connected to the Tc≡N^{2+} core. In this core, the nitride atom N^{3-}has made a complex with Tc (V) radiotrace. This nuclear medicine is a novel complex with a Tc≡N^{2+} core where the technetium (V) radionuclide is triple-bonded to a strong pi electron donor nitride atom and four donor sulfur atoms [24]. As it is evident from the Scheme 1, this radiopharmaceutical can be in three forms: anti, syn-endo and syn-exo isomers.

Structural study of the ^{99m}Tc-N(NOEt)$_2$ isomers

The density functional theory (DFT) method with B3LYP functional and cc-pVDZ//Lanl2DZ basis sets was used to optimize the molecular structure of anti, syn-endo and syn-exo isomers of bis(*N*-ethoxy-*N*-ethyl-dithiocarbamato)nitride technetium-99m radiopharmaceutical. The optimized structural geometries of all isomers are indicated in Figure 1. It can be seen from the Figure 1 that all three isomers have square pyramidal structure.

Figure 1. The theoretical geometric structures of ^{99m}Tc-N(NOEt)$_2$ isomers.

The bond length data of the isomers are listed in Table 1. It can be seen from the data that the Tc-N and Tc-S bond lengths of the structures are about 1.63-1.64 Å and 2.32-2.48 Å, respectively. Figure 2 shows the changes in bond lengths of the molecular structures. This curve indicates that changes in Tc-N bond length of the isomers are not tangible but changes in Tc-S bond lengths of the

structures are high. The changes in Tc-S bond lengths are due to the spatial positioning of ethoxy(ethyl)amino groups on ligands. Average amounts of Tc-S1, Tc-S2, Tc-S3 and Tc-S4 bond distances are 2.42 Å, 2.41 Å, 2.36 Å and 2.37 Å, respectively.

Table 1. Bond lengths data of the molecular structures.

Isomers	Tc-N	Tc-S1	Tc-S2	Tc-S3	Tc-S4
anti-^{99m}Tc-N(NOEt)$_2$	1.640	2.350	2.439	2.330	2.417
Syn-endo-^{99m}Tc-N(NOEt)$_2$	1.634	2.484	2.461	2.323	2.339
Syn-exo-^{99m}Tc-N(NOEt)$_2$	1.635	2.433	2.330	2.435	2.352

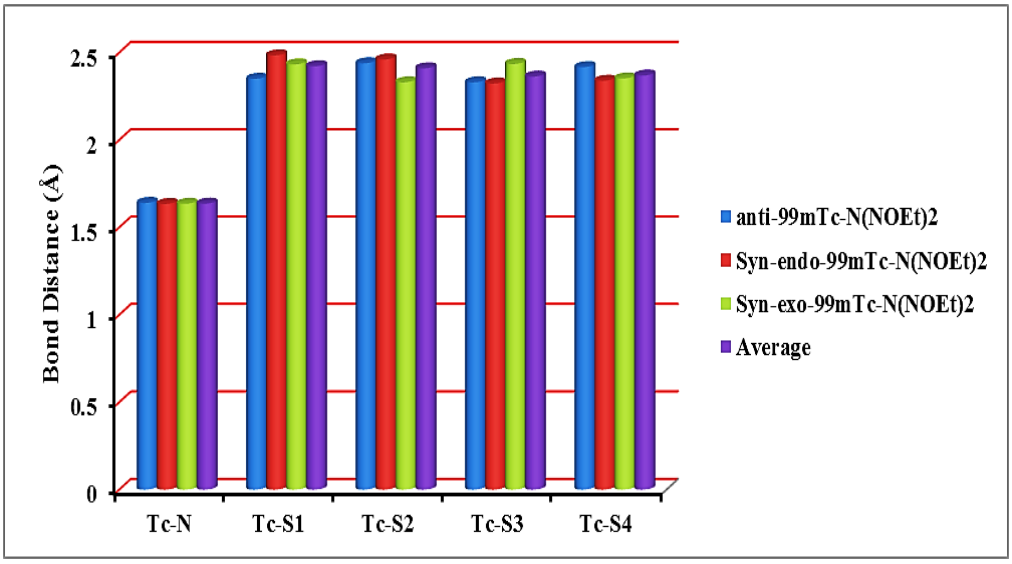

Figure 2. The bond lengths curve of ^{99m}Tc-N(NOEt)$_2$ isomers.

Table 2 shows the S-Tc-S and S-Tc-N bond angles data of the mentioned molecular structures. It can be seen from these data that the S-Tc-S bond angles of S-Tc-S-C rings are about 70 degree and 80 degree when the ethoxy(ethyl)amino groups on ligands are in positions endo and exo with Tc-N core, respectively. Also, the S-Tc-N bond angles data indicate that the all isomers of bis(*N*-ethoxy-*N*-ethyl-dithiocarbamato)nitride technetium-99m radiopharmaceutical don't have symmetrical squared pyramidal structure. This happens due to the steric pressure of the S-Tc-S-C rings. The variations in bond angles are shown in Figure 3. These variations will probably cause important differences in stability and reactivity properties of the molecular structures of the studied isomers. These properties will be discussed inthe next sections.

Table 2. Bond angles data of the molecular structures.

Angles	anti-^{99m}Tc-N(NOEt)$_2$	Syn-endo-^{99m}Tc-N(NOEt)$_2$	Syn-exo-^{99m}Tc-N(NOEt)$_2$

S1-Tc-S2	86.420	78.270	85.062
S2-Tc-S4	72.514	68.842	83.100
S1-Tc-S3	80.994	73.864	72.058
S3-Tc-S4	86.863	123.498	87.864
S1-Tc-N	121.497	98.771	102.871
S2-Tc-N	100.736	119.029	119.951
S3-Tc-N	121.792	111.991	102.210
S4-Tc-N	102.272	99.014	119.589

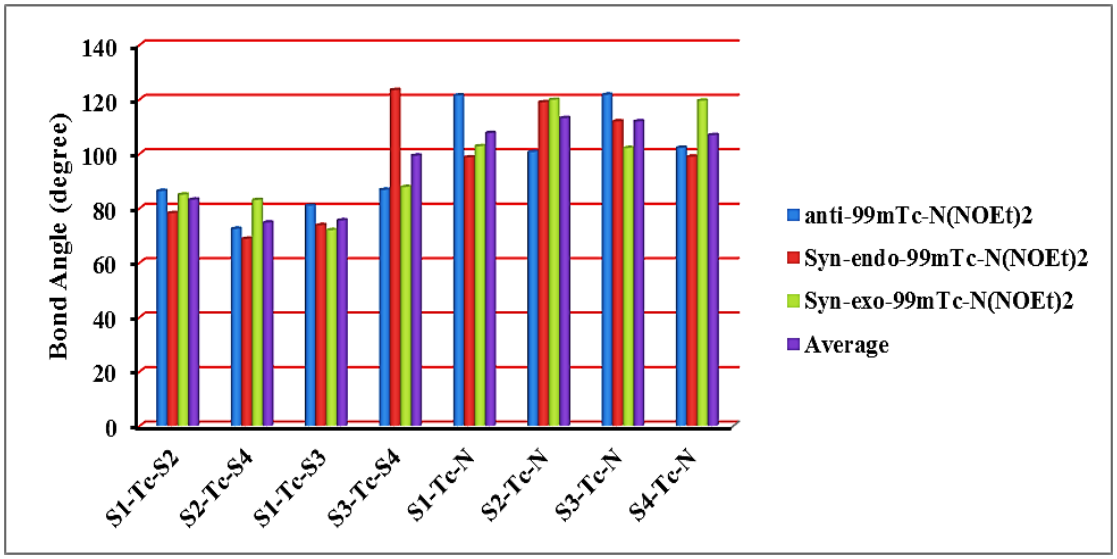

Figure 3. The bond angles curve of ^{99m}Tc-N(NOEt)$_2$ isomers.

From the data of the Table 3, the Tc-N and Tc-S bonds of all isomers are constructed from 2.3-2.4 and 0.6-0.7 bond orders, respectively. Figure 4 shows the differences in these bond orders in the mentioned molecular structures. We can see from the Figure 4 that these differences for each bond are negligible. So, the differences in the chemical properties of the isomers of ^{99m}Tc-N(NOEt)$_2$ radiopharmaceutical can't be related to the Tc-N and Tc-S bond orders.

Table 3. Bond orders (B.O.) data of the molecular structures.

Isomers	Tc-N	Tc-S1	Tc-S2	Tc-S3	Tc-S4
anti-^{99m}Tc-N(NOEt)$_2$	2.319	0.714	0.650	0.773	0.725
Syn-endo-^{99m}Tc-N(NOEt)$_2$	2.364	0.604	0.694	0.777	0.797
Syn-exo-^{99m}Tc-N(NOEt)$_2$	2.344	0.684	0.743	0.641	0.677

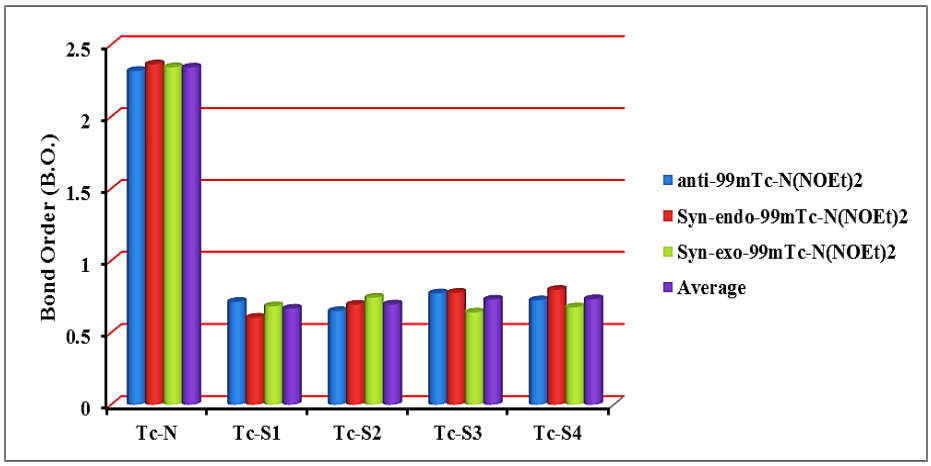

Figure 4. The bond orders curve of ^{99m}Tc-N(NOEt)$_2$ isomers.

Table 4 shows the data of the natural bond orbitals (NBOs) population analysis of all three isomers of ^{99m}Tc-N(NOEt)$_2$ nuclear medicine. The NBOs population analysis data gives us important information about the nature of Tc-N and Tc-S bonds of the studied molecular structures. From the data of the Table 4, more d orbitals of technetium atom and more p orbitals of nitrogen atom are participated in construction of the sigma and pi bonds of Tc≡N core of all three mentioned structures. In contrast, technetium atom uses more s and d orbitals in Tc-S bonds. So, this information indicates that the d orbitals of technetium atom play the main role to make the bonds with nitrogen and sulfur atoms.

Table 4. Natural bond orbital (NBO) population analysis data of the molecular structures.

Isomers	Bonds	Occupancy	Population/Bond orbital/Hybrids
anti-^{99m}Tc-N(NOEt)$_2$	σ(Tc-N)	1.97003	48.27% Tc ($sp^{0.22}d^{17.05}$), 51.73% N ($sp^{6.31}$)
	π1(Tc-N)	1.90674	53.77% Tc ($sp^{0.04}d^{15.72}$), 46.23% N (p)
	π2(Tc-N)	1.97426	59.73% Tc ($sp^{0.12}d^{76.47}$),40.27% N ($sp^{99.99}$)
	σ(Tc-S1)	1.85375	36.00% Tc ($sp^{0.04}d^{2.49}$), 64.00% S1 ($sp^{11.76}$)
	σ(Tc-S2)	1.93394	45.11% Tc ($sp^{0.08}d^{6.39}$), 54.89% S2 ($sp^{12.59}$)
Syn-endo-^{99m}Tc	σ(Tc-N)	1.92828	45.53% Tc ($sp^{0.14}d^{7.32}$), 54.47% N ($sp^{6.73}$)
	π1(Tc-N)	1.92251	53.77% Tc ($pd^{19.72}$), 47.24% N ($sp^{99.99}$)
	π2(Tc-N)	1.88008	55.50% Tc ($sp^{13.62}d^{99.99}$), 44.50% N (p)
	σ(Tc-S1)	1.78251	38.72% Tc ($sp^{0.22}d^{1.90}$), 61.28% S1 ($sp^{17.48}$)
Syn-exo-^{99m}Tc-	σ(Tc-N)	1.94176	48.02% Tc ($sp^{0.18}d^{9.80}$), 51.98% N ($sp^{6.56}$)
	π1(Tc-N)	1.68642	43.13% Tc ($sp^{99.99}d^{99.99}$), 56.87% N ($sp^{99.99}$)
	π2(Tc-N)	1.98386	58.19% Tc ($sp^{0.21}d^{99.99}$), 41.81% N ($sp^{99.99}$)
	σ(Tc-S1)	1.78951	36.71% Tc ($sp^{0.38}d^{2.03}$), 63.29% S1 ($sp^{13.30}$)

Stability and reactivity study of the ^{99m}Tc-N(NOEt)$_2$ isomers

The energies of frontier molecular orbitals (HOMO and LUMO) of the molecular structures of anti, syn-endo and syn-exo isomers of bis(*N*-ethoxy-*N*-ethyl-dithiocarbamato)nitride technetium-99m radiopharmaceutical have been listed in Table 5. Highly reactive compounds are related to the

molecular structures with low HOMO-LUMO energies gap. The lower the HOMO-LUMO energies gap, the easier the electron transition occurs [25-29]. It can be seen from the data of the Table 5 and density of states (DOS) graphs (Figure 5) that the reactivity order of molecular structures is: anti-^{99m}Tc-N(NOEt)$_2$(1.08 eV) >syn-exo-^{99m}Tc-N(NOEt)$_2$(1.24 eV) >syn-endo-^{99m}Tc-N(NOEt)$_2$(1.65 eV). The molecular electrostatic potential (MEP) graphs of the molecular structures (Figure 6) show how the density of electrons is distributed on the molecules. In these graphs, the red and blue loops are related to the electron-rich and electron-poor segments, respectively. The MEP graphs indicate that the electron-rich regions of the molecules are Tc-N and Tc-S bonds. This shows that the nucleophilic reagents can't react with ^{99m}Tc-N(NOEt)$_2$ isomers. So, all three molecular structures are stable. The relative stability of compounds is consistent with their binding energies [30-35]. Table 6 collects the binding energies data of the structures. We can easily see from the data that the relative stability of the studied molecular structures is: anti-^{99m}Tc-N(NOEt)$_2$>syn-endo-^{99m}Tc-N(NOEt)$_2$>syn-exo-^{99m}Tc-N(NOEt)$_2$. So, the ^{99m}Tc-N(NOEt)$_2$ nuclear medicine prefers the anti-position of ligands.

Table 5. Frontier molecular orbitals (FMOs) energies data of the molecular structures.

Isomers	HOMO (eV)	LUMO (eV)	GAP (eV)
anti-^{99m}Tc-N(NOEt)$_2$	-6.280	-5.200	1.080
Syn-endo-^{99m}Tc-N(NOEt)$_2$	-6.420	-4.770	1.650
Syn-exo-^{99m}Tc-N(NOEt)$_2$	-6.120	-4.880	1.240

Table 6. The binding energies data of the molecular structures.

Isomers	ΔE (kcal/mol)
anti-^{99m}Tc-N(NOEt)$_2$	972798.490
Syn-endo-^{99m}Tc-N(NOEt)$_2$	972793.244
Syn-exo-^{99m}Tc-N(NOEt)$_2$	972792.853

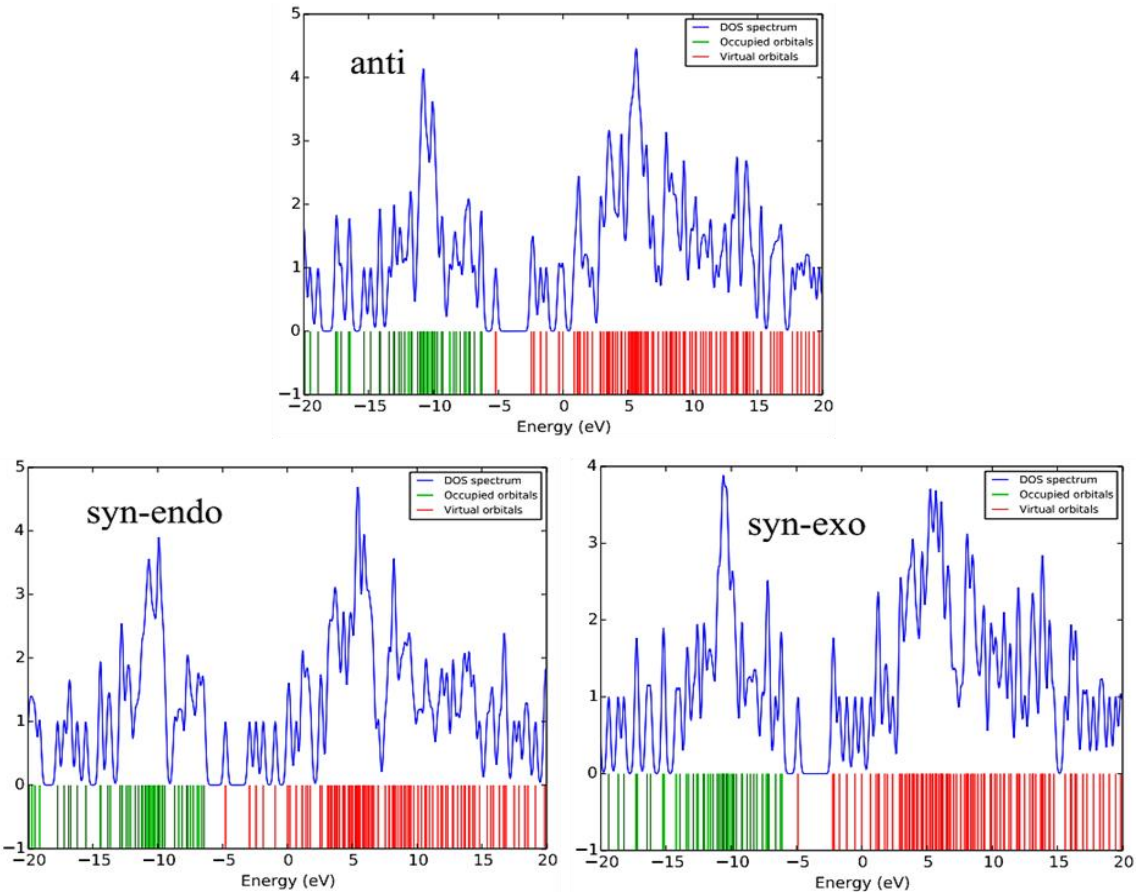

Figure 5. The density of states (DOS) graphsof ^{99m}Tc-N(NOEt)$_2$ isomers.

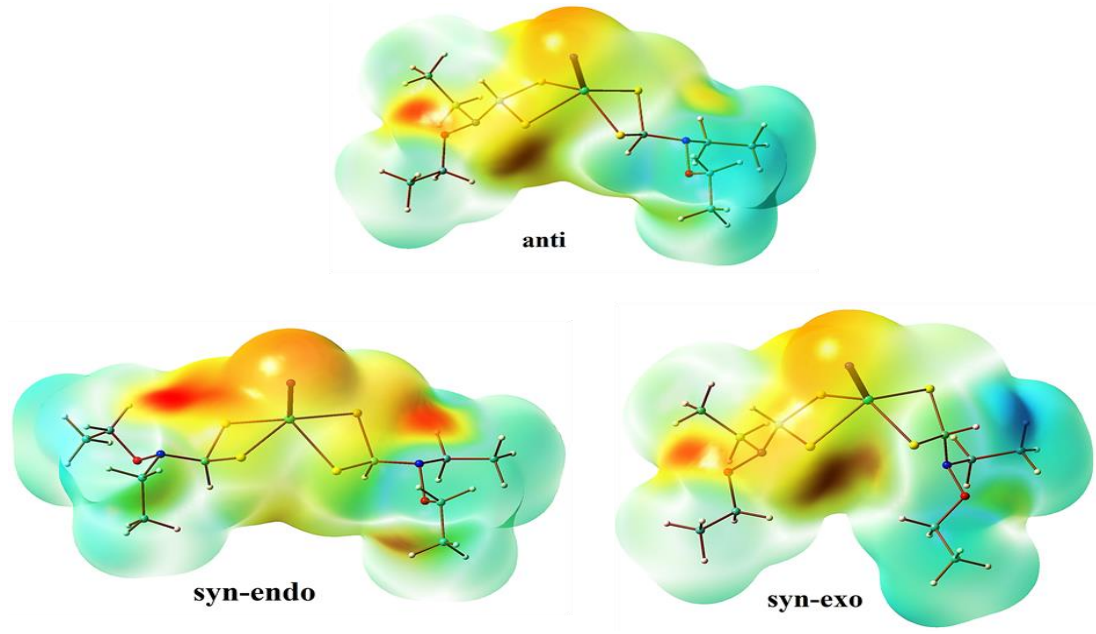

Figure 6. The molecular electrostatic potential (MEP) graphsof ^{99m}Tc-N(NOEt)$_2$ isomers.

Spectral study of the ^{99m}Tc-N(NOEt)$_2$ isomers

There are several spectroscopic techniques which can be used to identify organic molecules: infrared (IR), mass spectroscopy (MS), UV-Visible spectroscopy (UV-Vis) and nuclear magnetic resonance (NMR) [36-38]. Figures 7-9 are related to the CD, IR and UV-Vis spectra, respectively.

Circular dichroism (CD) spectroscopy is a light absorption spectroscopy method that measures the difference in absorbance of right- and left-circularly polarized light (rather than the commonly used absorbance of isotropic light) by a substance. The CD of molecules is measured over a range of wavelengths and is used to chiral molecules of all types and sizes. Measurements performed in the ultra-violet and visible regions of the electro-magnetic spectrum monitor electronic transitions, and, if the molecule under study contains chromophores then one circularly polarized light (CPL) state will be absorbed to a greater extent than the other and the CD signal over the corresponding wavelengths will be non-zero. A CD signal can be positive or negative, depending on whether L-CPL is absorbed to greater extent than R-CPL (CD signal positive) or to a lesser extent (CD signal negative) [39-43]. So, It can be seen from the graphs of the Figure 7 that the anti-^{99m}Tc-N(NOEt)$_2$ and syn-exo-^{99m}Tc-N(NOEt)$_2$ structures show R-CPL state and the syn-endo-^{99m}Tc-N(NOEt)$_2$molecular structure indicates L-CPL state.

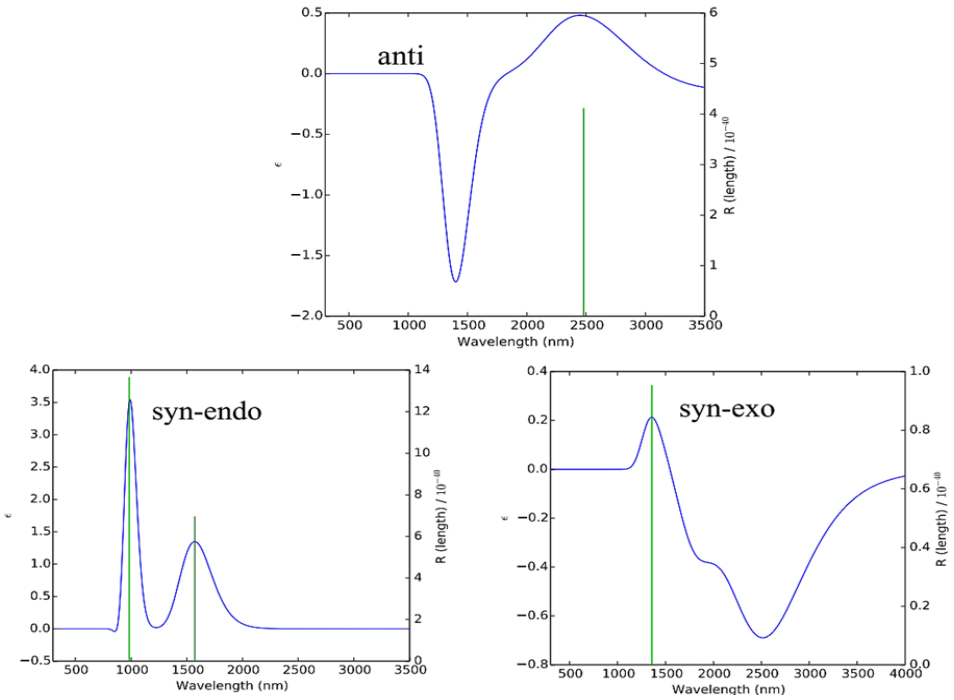

Figure 7. The CD spectraof ^{99m}Tc-N(NOEt)$_2$ isomers.

Figure 8 shows the IR spectra of the molecular structures under study. Here, the main harmonic frequencies (cm^{-1}) of the structures are discussed.

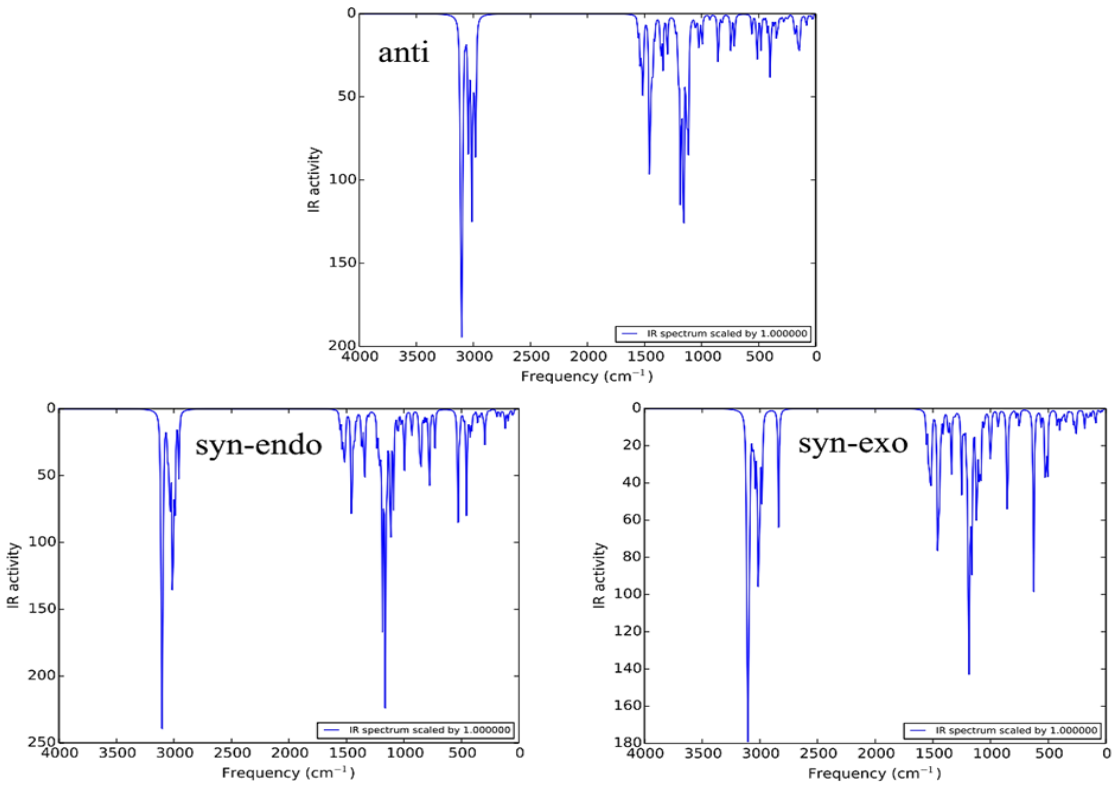

Figure 8. The IR spectra of ^{99m}Tc-N(NOEt)$_2$ isomers.

anti-^{99m}Tc-N(NOEt)$_2$: 28.13, 51.89, 78.82, 86.58, 94.16, 111.55, 136.47, 140.74, 149.21, 152.88, 160.69, 180.74, 187.17, 192.71, 244.67, 259.54, 277.43, 286.79, 302.07, 302.53, 309.32, 325.57, 333.01, 341.44, 343.94, 366.44, 383.84, 398.45, 403.92, 424.67, 450.34, 479.49, 510.84, 518.27, 558.85, 711.65, 738.35, 743.01, 813.84, 821.69, 837.87, 852.13, 855.68, 859.56, 863.07, 926.22, 929.88, 996.58, 1022.97, 1047.79, 1055.74, 1115.80, 1116.82, 1123.93, 1133.39, 1155.10, 1159.67, 1166.55, 1182.19, 1187.06, 1189.77, 1203.64, 1204.86, 1207.89, 1213.11, 1228.83, 1300.72, 1306.03, 1306.43, 1339.96, 1356.64, 1362.29, 1410.47, 1426.99, 1430.79, 1436.55, 1446.71, 1453.75, 1457.39, 1458.06, 1510.17, 1510.32, 1512.34, 1516.74, 1518.29, 1525.32, 1530.11, 1531.22, 1538.41, 1538.77, 1556.46, 1557.08, 2977.28, 2977.47, 2982.79, 2994.61, 3009.45, 3010.91, 3011.41, 3014.22, 3014.99, 3025.85, 3040.59, 3044.83, 3067.34, 3081.31, 3091.98, 3100.59, 3101.54, 3103.81, 3104.54, 3108.13, 3112.08, and 3115.22.

syn-endo-^{99m}Tc-N(NOEt)$_2$: 43.44, 52.82, 83.80, 88.00, 96.80, 111.10, 115.76, 120.91, 140.08, 145.92, 162.65, 179.13, 190.33, 193.79, 252.77, 259.49, 280.71, 287.60, 297.37, 300.54, 307.73, 313.18, 336.44, 341.21, 346.62, 359.10, 388.46, 397.63, 410.94, 426.23, 455.37, 481.60, 516.25, 530.45, 530.66, 730.99, 779.76, 784.55, 809.36, 824.66, 827.95, 952.93, 861.17, 861.88, 867.49, 930.44, 932.81, 996.11, 1023.72, 1053.83, 1091.03, 1116.48, 1117.04, 1124.77, 1145.70, 1161.94, 1164.58,

1183.37, 1186.92, 1188.08, 1205.56, 1207.02, 1207.23, 1214.62, 1220.97, 1233.94, 1305.01, 1306.52, 1340.97, 1345.84, 1360.11, 1367.14, 1409.93, 1428.06, 1431.57, 1438.31, 1447.92, 1451.43, 1457.26, 1457.41, 1509.42, 1510.44, 1510.71, 1517.86, 1518.41, 1523.93, 1530.80, 1531.21, 1538.38, 1538.53, 1556.46, 1559.31, 2957.30, 2989.15, 3002.64, 3003.24, 3009.06, 3011.93, 3012.10, 3015.01, 3032.16, 3032.90, 3039.90, 3048.29, 3056.17, 3074.12, 3092.99, 3101.30, 3102.76, 3103.04, 3104.26, 3105.28, 3111.90, and 3112.04.

syn-exo-^{99m}Tc-N(NOEt)$_2$: 29.99, 51.21, 86.03, 86.33, 88.35, 93.12, 97.17, 126.83, 144.69, 150.31, 161.38, 185.05, 195.39, 220.45, 259.88, 276.31, 279.47, 283.50, 284.04, 301.14, 303.02, 313.90, 332.13, 340.61, 348.76, 367.66, 381.10, 388.01, 401.81, 422.56, 438.16, 507.04, 516.68, 525.62, 561.08, 626.41, 750.18, 777.51, 814.56, 827.28, 841.64, 853.70, 855.58, 862.88, 864.02, 930.33, 935.82, 996.89, 1004.92, 1055.37, 1085.46, 1100.24, 1117.57, 1118.49, 1124.95, 1126.26, 1161.26, 1166.84, 1184.30, 1185.69, 1191.62, 1197.36, 1206.15, 1208.05, 1209.39, 1230.20, 1251.77, 1304.13, 1312.17, 1339.94, 1362.44, 1369.41, 1409.85, 1411.33, 1430.00, 1436.51, 1445.62, 1448.10, 1457.03, 1460.30, 1510.12, 1511.33, 1516.16, 1517.19, 1524.24, 1524.42, 1530.55, 1531.70, 1535.93, 1539.06, 1554.33, 1558.58, 2837.07, 2979.84, 2985.99, 2998.21, 3009.70, 3010.11, 3010.84, 3014.15, 3023.51, 3038.15, 3043.77, 3057.04, 3065.06, 3083.43, 3090.74, 3098.40, 3100.43, 3103.21, 3105.39, 3107.97, 3110.56, and 3114.61.

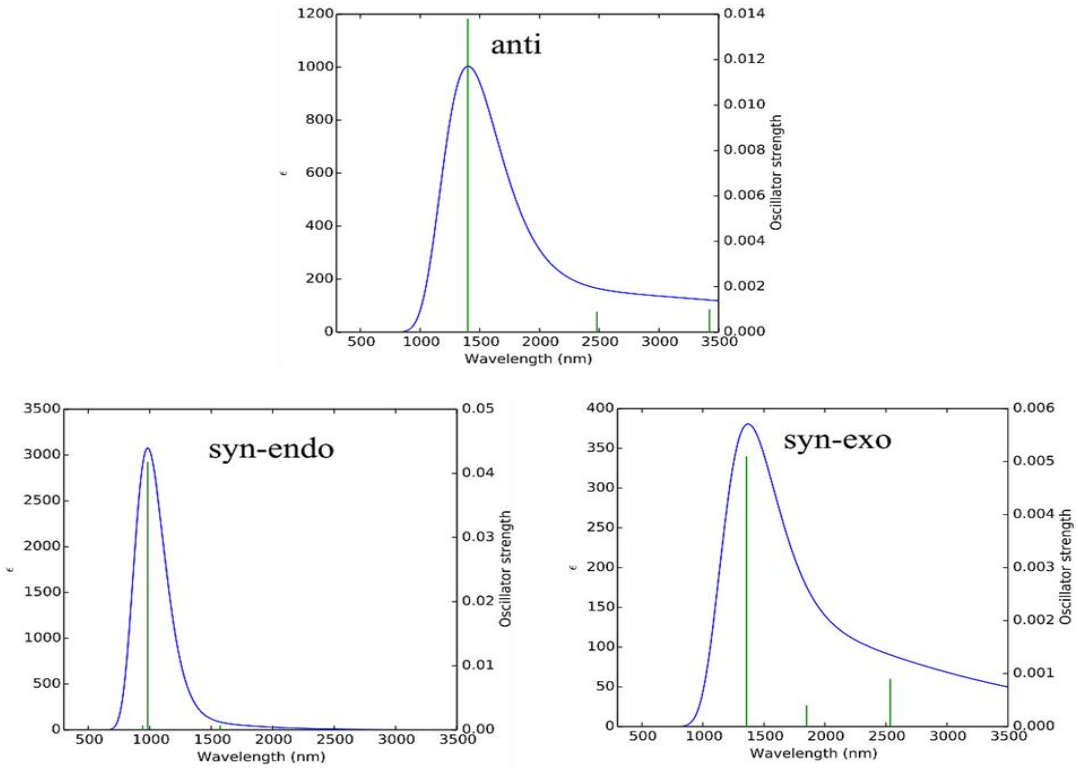

Figure 9. The UV-Vis spectraof ^{99m}Tc-N(NOEt)$_2$ isomers.

The UV-Vis spectrum is one of the most important methods in determining the chemical properties of organic-inorganic compounds [44-47]. Here, the electronic transitions of the studied molecular structures are discussed (Figure 9). All three isomers don't show any electronic transition at ultra-violet wavelengths region.

anti-^{99m}Tc-N(NOEt)$_2$: UV-Vis [wavelength of electronic transition (nm), energies (cm^{-1}), electronic transitions]:

a. 3424.008 nm (2920.554cm^{-1}), HOMO-1 to LUMO (15%) and HOMO to LUMO (42%)

b. 2480.163 nm (4031.993cm^{-1}), HOMO-1 to LUMO (49%) and HOMO to LUMO (38%)

c. 1400.625 nm (7139.669cm^{-1}), HOMO-2 to LUMO (74%)

syn-endo-^{99m}Tc-N(NOEt)$_2$: UV-Vis [wavelength of electronic transition (nm), energies (cm^{-1}), electronic transitions]:

a. 1571.598 nm (6362.076cm^{-1}), HOMO-1 to LUMO (23%) and HOMO to LUMO (66%)

b. 983.761 nm (10165.076cm^{-1}), HOMO-1 to LUMO (59%) and HOMO to LUMO (19%)

c. 942.982nm (10604.651cm^{-1}), HOMO-3 to LUMO (62%), HOMO-2 to LUMO (22%), HOMO-5 to LUMO (2%) and HOMO-1 to LUMO (3%)

syn-exo-^{99m}Tc-N(NOEt)$_2$: UV-Vis [wavelength of electronic transition (nm), energies (cm^{-1}), electronic transitions]:

a. 2534.928 nm (3944.885cm^{-1}), HOMO-1 to LUMO (20%) and HOMO to LUMO (55%)

b. 1849.393 nm (5407.178cm^{-1}), HOMO-1 to LUMO (59%) and HOMO to LUMO (33%)

c. 1357.531nm (7366.312cm^{-1}), HOMO-2 to LUMO (84%)

Conclusion

The main aimof the present paper is to discuss the stability, reactivity, structural and spectral properties of the anti, syn-endo and syn-exo isomers of bis(*N*-ethoxy-*N*-ethyl-dithiocarbamato)nitride technetium-99m radiopharmaceutical. The study was conducted based on the quantum-mechanical computations. The studied molecular structure was optimized by B3LYP/cc-pVDZ basis set of theory. The Lanl2DZ basis set was used for the computation of technetium-99m radionuclide. From the computations and mathematical calculations, the following conclusions were drawn.

1. Two (ethoxy(ethyl)amino)methanedithiol ligands have been connected to the Tc≡N^{2+} core.

2. The changes in Tc-N bond length of the isomers aren't tangible but changes in Tc-S bond lengths of the structures are high. The changes in Tc-S bond lengths are due to the spatial positioning of ethoxy(ethyl)amino groups on ligands.

3. All three isomers don't have symmetrical squared pyramidal structure.

4. The differences in the chemical properties of the isomers of ^{99m}Tc-N(NOEt)$_2$ radiopharmaceutical can't be related to the Tc-N and Tc-S bond orders.

5. The d orbitals of technetium atom play the main role to make the bonds with nitrogen and sulfur atoms.

6. The reactivity order of molecular structures is: anti-^{99m}Tc-N(NOEt)$_2$>syn-exo-^{99m}Tc-N(NOEt)$_2$>syn-endo-^{99m}Tc-N(NOEt)$_2$.

7. All three molecular structures are stable but the relative stability of the studied molecular structures is: anti-^{99m}Tc-N(NOEt)$_2$>syn-endo-^{99m}Tc-N(NOEt)$_2$>syn-exo-^{99m}Tc-N(NOEt)$_2$.

8. The nucleophilic reagents can't react with ^{99m}Tc-N(NOEt)$_2$ isomers.

9. From the CD spectra, the anti-^{99m}Tc-N(NOEt)$_2$ and syn-exo-^{99m}Tc-N(NOEt)$_2$ structures show R-CPL state and the syn-endo-^{99m}Tc-N(NOEt)$_2$ molecular structure indicates L-CPL state.

10. All three isomers don't show any electronic transition at ultraviolet wavelengths region.

Acknowledgements:

The corresponding author is grateful to Mr. HosseinAbbasi for providing valuable suggestions.

References

[1]. Nabati M., Mahkam M. *Iran Chem. Commun.,* 2014, **2:**129

[2]. Fagret D., Ghezzi C., Vanzetto G. *J. Nucl. Med.,* 2001, **42:**1395

[3]. Hatada K., Riou L.M., Ruiz M., Yamamichi Y., Duatti A., Lima R.L., Goode A.R., Watson D.D., Beller G.A., Glover D.K. *J. Nucl. Med.,* 2004, **45:**2095

[4]. Nabati M. *Iran. J. Org. Chem.,* 2017, **9:**2045

[5]. Takahana K., Beller G.A., Ruiz M., Petruzella F.D., Watson D.D., Glover D.K. *J. Nucl. Med.,* 2001, **42:**1388

[6]. Nabati M., Salehi H. *Iran. J. Org. Chem.,* 2017, **9:**2013

[7]. Nabati M., Mofrad M.H., Kermanian M., Sarshar S. *Iran. J. Org. Chem.,* 2017, **9:**1981

[8]. Nabati M., Kermanian M., Maghsoudloo-Mahalli A., Sarshar S. *Iran. J. Org. Chem.,* 2017, **9:**2067

[9]. Hernandez-Valdes D., Blanco-Gonzalez A., Garcia-Fleitas A., Rodriguez-Riera Z., Meola G., Alberto R., Jauregui-Haza U. *J. Mol. Graph. Model.,* 2017, **71:**167

[10]. Lamb J., Holland J.P. *J. Nucl. Med.,* 2018, **59:**382

[11]. Dijk J.D.V., Jager P.L., Osch J.A.C.V., Dalen J.A.V. *J. Nucl. Med.,* 2017, **58:**518

[12]. Nabati M., Kermanian M., Mohammadnejad-Mehrabani H., Kafshboran H.R., Mehmannavaz M., Sarshar S. *Chem. Method.,* 2018, **3:**132

[13]. Nabati M. *Chem. Method.,* 2017, **2:**128

[14]. Hernandez-Valdes D., Alberto R., Jauregui-Haza U. *RSC Adv.,* 2016, **6:**107127

[15]. Nabati M. *Iran. J. Org. Chem.,* 2018, **10:**2291

[16]. Renaud J.M., Yip K., Guimond J., Trottier M., Pibarot P., Turcotte E., Maguire C., Lalonde L., Gulenchyn K., Farncombe T., Wisenberg G., Moody J., Lee B., Port S.C., Turkington T.G., Beanlands R.S., DeKemp R.A. *J. Nucl. Med.,* 2017, **58:**103

[17]. Nabati M., Maghsoudloo-Mahalli A., Mohammadnejad-Mehrabani H., Movahed-Tazehkand H. *Iran. J. Org. Chem.,* 2018, **10:**2281

[18]. Cittanti C., Uccelli L., Pasquali M., Boschi A., Flammia C., Bagatin E., Casali M., Stabin M.G., Feggi L., Giganti M., Duatti A. *J. Nucl. Med.,* 2008, **49:**1299

[19]. Nabati M., Maghsoudloo-Mahalli A. *Iran. J. Org. Chem.,* 2017, **9:**2239

[20]. Bolzati C., Cavazza-Ceccato M., Agostini S., Refosco F., Yamamichi Y., Tokunaga S., Carta D., Salvarese N., Bernardini D., Bandoli G. *Bioconjugate Chem.,* 2010, **21:**928

[21]. Nabati M., Mohammadnejad-Mehrabani H. *Iran. J. Org. Chem.,* 2017, **9:**2117

[22]. Maria L., Soares M., Santos I.C., Sousa V.R., Mora E., Marcalo J., Luzyanin K.V. *Dalton Trans.,* 2016, **45:**3778

[23]. Nabati M., Mahkam M. *Org. Chem. Res.,* 2016, **2:**70

[24]. Nabati M. *Iran. J.Org. Chem.,* 2016, **8:**1935

[25]. Nabati M., Mahkam M. *J. Phys. Theor. Chem.,* 2015, **12:**121

[26]. Nabati M. *J. Phys. Theor. Chem.,* 2015, **12:**325

[27]. Nabati M. *J. Phys. Theor. Chem.,* 2017, **14:**49

[28]. Nabati M., Mahkam M. *J. Phys. Theor. Chem.,* 2015, **12:**33

[29]. Nabati M., Mahkam M., Atani Y.G. *J. Phys. Theor. Chem.,* 2016, **13:**35

[30]. Nabati M. *J. Phys. Theor. Chem.,* 2016, **13:**133

[31]. Moura C., Gano L., Mendes F., Raposinho P.D., Abrantes A.M., Botelho M.F., Santos I., Paulo A. *Eur. J. Med. Chem.,* 2012, **50:**350

[32]. Nabati M., Mahkam M. *Inorg. Chem. Res.,* 2016, **1:**131

[33]. Nabati M., Mahkam M. *Silicon,* 2016, **8:**461

[34]. Nabati M. *Iran. J. Org. Chem.,* 2015, **7:**1631

[35]. Qian W., Zhang W., Zong H., Gao G., Zhou Y., Zhang C. *J. Mol. Model.,* 2016, **22:**9

[36]. Nabati M. *Iran. J. Org. Chem.,* 2015, **7:**1669

[37]. Nabati M. *Iran. J. Org. Chem.,* 2016, **8:**1703

[38]. Nabati M., Hojjati M. *Iran. J. Org. Chem.,* 2016, **8:**1777

[39]. Nabati M. *Iran. J. Org. Chem.,* 2016, **8:**1803

[40]. Nabati M. *Iran. J. Org. Chem.,* 2016, **8:**1817

[41]. Maurer R.I., Blower P.J., Dilworth J.R., Reynolds C.A., Zheng Y., Mullen G.E.D. *J. Med. Chem.,* 2002, **45:**1420

[42]. Gancheff J., Kremer C., Kremer E., Ventura O.N. *J. Mol. Struct: THEOCHEM,* 2002, **580:**107

[43]. Okoye C.M.I. *J. Phys: Condens. Matter.,* 2003, **15:**5945

[44]. Zhang Y., Sun Y., Xu X., Zhang X., Zhu H., Huang L., Qi Y., Shen Y. *J. Med. Chem.,* 2010, **53:**3262

[45]. Banerjee P., Sproules S., Weyhermuller T., George S.D., Wieghardt K. *Inorg. Chem.,* 2009, **48:**5829

[46]. Gong Y., Zhou M., Andrews L. *Chem. Rev.,* 2009, **109:**6765

[47]. Sproules S., Benedito F.L., Bill E., Weyhermuller T., George S.D., Wieghardt K. *Inorg. Chem.,* 2009, **48:**10926

How to cite this manuscript: Mehdi Nabati*. Insight into the stability, reactivity, structural and spectral properties of the anti, syn-endo and syn-exo isomers of bis(*N*-ethoxy-*N*-ethyl-dithiocarbamato)nitrido technetium-99m [^{99m}Tc-N(NOEt)$_2$] radiopharmaceutical. Chemical Methodologies 2(3), 2018, 223-238. DOI: 10.22631/chemm.2018.125281.1043.